Investigation of Removal Mechanism of 4H-SiC and 6H-SiC Substrates Using Molecular Dynamics Simulation

Zige Tian[1,2]**, Xun Chen**[2] **and Xipeng Xu**[1]

[1] Institute of Manufacturing Engineering, Huaqiao University, Xiamen, 361021, Fujian Province, P.R. China
[2] Faculty of Engineering and Technology, Liverpool John Moores University, L3 3AF, Liverpool, United Kingdom

X.Chen@ljmu.ac.uk

Abstract. Single crystal silicon carbide (SiC) is widely used in semiconductor devices and illumination devices. The anisotropic characteristics of SiC crystal structure presents different physical properties on the C face and Si face of a single crystal silicon carbide leading to different applications. Aiming at the understanding of the mechanism of material removal and subsurface defect, this paper presents the molecular dynamics simulations of scratching on the C face and Si face of 4H-SiC and 6H-SiC materials. The results show that the material removal at the C face is easier than that at the Si face, so that less subsurface amorphous deformation appears on the C face. Such a difference is due to a key phenomenon - the dislocations on the basal plane (0001) in the SiC subsurface during scratching.

1. Introduction

Single crystal silicon carbide (SiC) plays very important roles in many engineering applications because of some excellent properties, such as high thermal conductivity and stability, high stiffness and good chemical inertness [1]. Within different polytypes of SiC, 4H-SiC have wide applications for optoelectronics, high-temperature electronics, high-performance mirrors and micro/nano dies; while 6H-SiC is mainly used for optoelectronic devices, such as diodes for laser and blue light emitting [2-5]. These ultra-precision micro/nano components require damage-free atomically smooth surfaces, because any nanoscale defects either derived from the material growth or produced from the machining process are harmful to SiC-based devices [6]. Thus, the investigation of the nanoscale mechanical properties and material removal mechanism of 4H-SiC and 6H-SiC substrates is of great interests and significance, therefore it has attracted a lot of attention in research community. Scholars have undertaken indentation and scratching experiments, which are common methods to study the nanomechanical properties of on 4H-SiC and 6H-SiC. Indentation load-displacement curves could show the material deformation transition conditions between elastic, plastic and fracture. Researches [7, 8] demonstrated the yielding or incipient plasticity of 4H-SiC and 6H-SiC at a pop-in event are of a shear stress of about 21 GPa and 23.4 GPa. Grim et al. [9] experimentally confirmed that basal dislocation could appear in the subsurface of 6H-SiC during mechanical polishing.

It is difficult to observe nanoscale phenomena experimentally, while molecular dynamics (MD) can be applied effectively to illustrate the movement and interaction of molecules or atoms and to allow the material deformation and removal mechanism during indentation and scratching on 4H-SiC and

6H-SiC to be investigated. Goel et al. [10] compared the material behaviours of 3C-SiC, 4H-SiC and 6H-SiC in nanocutting and found the subsurface integrity of 4H-SiC was better than others. In fact, 6H-SiC showed the worst. Wu et al. [11] analysed the deformation of 6H-SiC during nano-cutting and convinced the structural transformation in 6H-SiC was an amorphous transformation. Meanwhile, the dislocations could occur in subsurface and their migration would lead to a stacking fault in the basal plane. Although these MD simulations can analyse the material removal mechanisms and phenomena qualitatively at nanoscale, it is still difficult to provide specified quantitative guidance for actual machining.

Further, the anisotropy of single crystal 4H-SiC and 6H-SiC presents different physical and chemical properties at the Si face and C face and therefor they are suitable for different commercial applications [12-14]. The majority of previous researches focus on the Si face [15-17], less are on the C face [18]. There are still few researches on this anisotropy in nanoscale machining. Considering the chemical reactions on the sample surface, Chen et al. [19] found the material removal rate (MRR) of Si face was higher than that of C face during polishing, because the oxidized Si face was easily removed. However, in contrast, Lu et al. [20, 21] reported that MRR on the C face was higher, and considered the MRR diversity was caused by the mechanical properties of different faces. Yagi et al. [22] also reported that the Si face is more difficult to cut than the C face. Therefore, a fundamental understanding of the material removal mechanism of 4H-SiC and 6H-SiC is inevitable and critical for the explanation of the different MRR between Si face and C face and for improving the efficiency and quality of SiC polishing.

This paper presents an investigation of the material removal mechanism of 4H-SiC and 6H-SiC scratching using MD simulations, which reveals the reasons for the differences between Si face and C face. The investigation finding sets a good theoretical foundation that could guide SiC polishing practice.

2. Models of MD simulation for abrasive scratching

As shown in Figure 1, the models of 4H-SiC or 6H-SiC workpieces contain around 923 thousand within the space of 40 nm × 19.7 nm × 12 nm (length × width × height). While the fixed boundary condition is applied in x- and z-directions, the periodic boundary condition is used in y-direction. The cutting edge of the abrasive grit is designed as a rigid hollow hemisphere on a cylinder column of radius 5 nm.

The workpiece consists three layers, i.e. the Newtonian atoms (NVE ensemble), the thermostatic atomic layer (NVT ensemble) and the boundary atomic layer. The main body of the workpiece are Newtonian atoms that follow the classic Newton's law of motion, which are commonly used scratching simulation [23-25]. The boundary atomic layer can hold the workpiece and prevent the rigid movement during scratching. The thermostatic atomic layer provides a control to limit the workpiece temperature within a specified range using a Berendsen thermostat, which can absorb the heat generated from the Newtonian atoms by adjusting the atomic velocity during scratching. In addition, the atoms in the cutting edge are set as rigid bodies based on the fact that diamond is much harder than both 4H-SiC and 6H-SiC.

To ensure the MD simulation accuracy and reliability, the selection of potential function for the MD analysis is a critical issue. A three-body potential function - Tersoff potential function is selected for this investigation, because it provides a more realistic description of covalent bonded materials [26]. Here, the interaction between C-C, Si-Si, and Si-C atoms are presented with the Tersoff potential function as follows:

$$\mathrm{E} = \frac{1}{2} \sum_i \sum_{j \neq i} \mathrm{V}_{ij} \tag{1}$$

$$\mathrm{V}_{ij} = f_C(r_{ij})[f_R(r_{ij}) + \mathrm{b}_{ij} f_A(r_{ij})] \tag{2}$$

$$f_C(r) = \begin{cases} 0 & : \ r < R - D \\ \frac{1}{2} - \frac{1}{2}\sin\left(\frac{\pi}{2}\frac{r-R}{D}\right) & : \ R - D < r < R + D \\ 1 & : \ r > R + D \end{cases} \quad (3)$$

$$f_R(r) = \mathrm{A}\exp(-\lambda_1 r) \quad (4)$$

$$f_A(r) = -\mathrm{B}\exp(-\lambda_2 r) \quad (5)$$

$$b_{ij} = (1 + \beta^n {\zeta_{ij}}^n)^{-\frac{1}{2n}} \quad (6)$$

$$\zeta_{ij} = \sum_{k \neq i,j} f_C(r_{ik}) g(\theta_{ijk}) \exp\left[{\lambda_3}^m (r_{ij} - r_{ik})^m\right] \quad (7)$$

$$g(\theta) = \gamma_{ijk}\left(1 + \frac{c^2}{d^2} - \frac{c^2}{[d^2 + (cos\theta - cos\theta_0)^2]}\right) \quad (8)$$

Where E is the total energy, the sub-function V_{ij} describes the energy between two atoms (i and j), (i, j and k) label the three atoms of the system, f_R represents a repulsive pair potential, f_A represents an attractive pair potential, f_C represents a smooth cutoff function to limit the range of the potential, r_{ij} is the length of the i-j bond, b_{ij} is the bond order term, ζ_{ij} counts the number of other bonds to atom i besides the i-j bond, θ_{ijk} is the bond angle between the bonds i-j and i–k and $\chi_{Si–C}$ is the mixing parameter [10].

In this investigation, the abrasive scratching was conducted on the basal plane (0001) that is perpendicular to z axis along the direction [1-210], i.e. the x axis. The scratching conditions are set as: the speed is 100 m/s and the depth is 3 nm. The thermostatic layer controls the temperature at 300 K during the simulation, and a 150 ps relaxation process of the system is conducted before the simulations start. The time step of 1 fs was selected for the simulation. All MD simulations here were conducted and analysed by using a software platform of large-scale atomic/molecular massively parallel simulator (LAMMPS) [27]. In addition, the occurrences of deformation and dislocation during scratching can be detected by using the dislocation extraction algorithm (DXA) [28]. Once simulation finished, the MD results are visually presented by using OVITO [29].

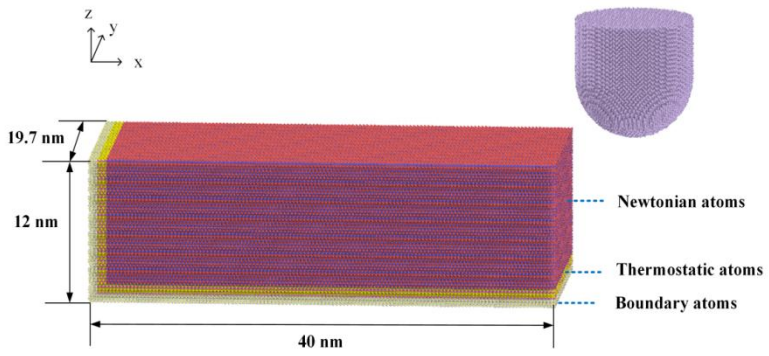

Figure 1. MD scratching model.

3. MD simulation for abrasive scratching and its validation

The MD model used in this investigation has been verified experimentally by the experiments of indentation and scratching that were previously reported in the literature [30]. By comparing the results of indentation and scratching on 4H-SiC and 6H-SiC, it was found that the phenomena of the MD simulation are of the same trend of the experimental results, therefore, the MD model was considered to be reliable. In addition, this MD model will also be verified in this paper in terms of workload pressure and MMR.

Due to the practical difficulties to conduct experiments in the same scale of MD simulation, for example, the size of abrasive cutting edge tip used in scratching scales, directly compare the results between the simulation and experiment will inevitably involves in error. Therefore, the validation is mainly focus on qualitative trends that show the influence of each conditional parameter. To compare scratching behaviours within the MD simulations and experiments, the loading pressure, defined as acting force/contact area, is used. As shown in Figure 2, the acting forces in MD simulations are taken from the scratching cutting edge tip, which are the average tangential and normal forces taken from the stable stages of scratching processes. For MD simulations, the scratching depth keeps as a constant (3 nm). For scratching experiments, a constant normal scratching load (4 mN) was applied and the average displacements in the normal direction were measured during the stable scratching stages. It is interesting to see that the loading pressures of scratching C face are lower than those of scratching Si face, and the loading pressures on 4H-SiC are greater than those on 6H-SiC. Due to the difference in scratching tip sizes (5 nm in the MD simulations and 3 μm in the experiments), the loading pressure are significantly different, however, the variation trends are consistent in both simulations and experiments. This convinces the MD simulation could provide a meaningful evidence for the interpretation of the scratching behaviours.

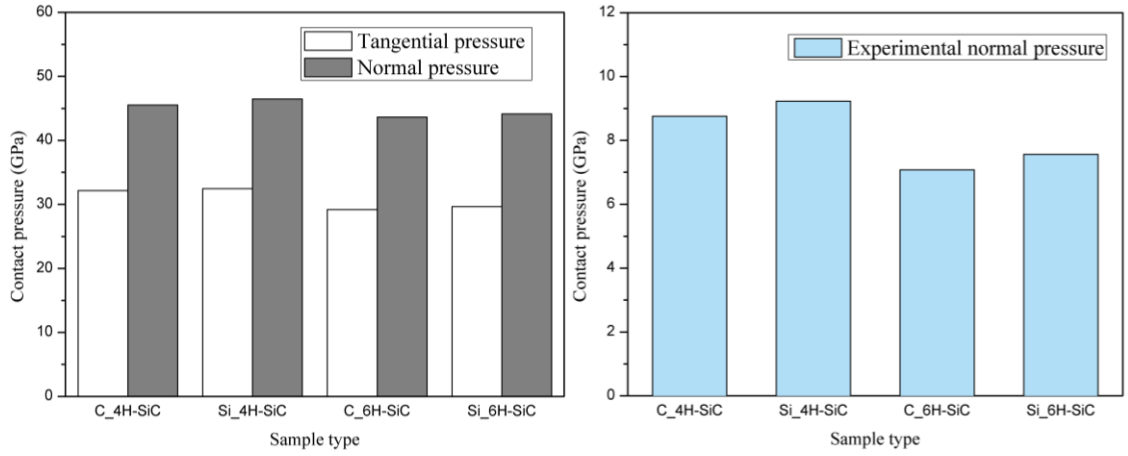

Figure 2. (a) Contact pressure of MD simulations. (b) Contact pressure of scratching experiments [30]

High material removal rate (MRR) is a desirable characteristics of a machining process. As a key measure to evaluate the machining process efficiency, the MRR plays an important role in the MD simulation analysis. The atoms, which positions are higher than the workpiece original surface after the scratching tip passed, are considered as atom displacement due to scratching and often used to present the scratching material removal. However, this may not actually present real materials removal. Look at the grit-workpiece interaction region, as shown in Figure 3 (a), the bulged atoms on both sides along the scratching path forming ridges as the results of "ploughing" action will stay on the workpiece, so they should not be considered as material removal. Only those atoms whose positions are higher than the ploughing ridge height can be considered as potential finally removed atoms. From Figures 3 (b) and (c), the atom displacements in various scratching tests show that the number of potential finally removed atoms is much smaller than that of total atoms above the original workpiece surface. This means only small proportion of displaced atoms will be removed by scratching, and significant energy has been consumed in deforming materials without actually contributing material removal. Further through observation, a higher MRR shows at the C face of SiC than that at the Si face, which is similar to the experimental results previous research demonstrated by Luo [20].

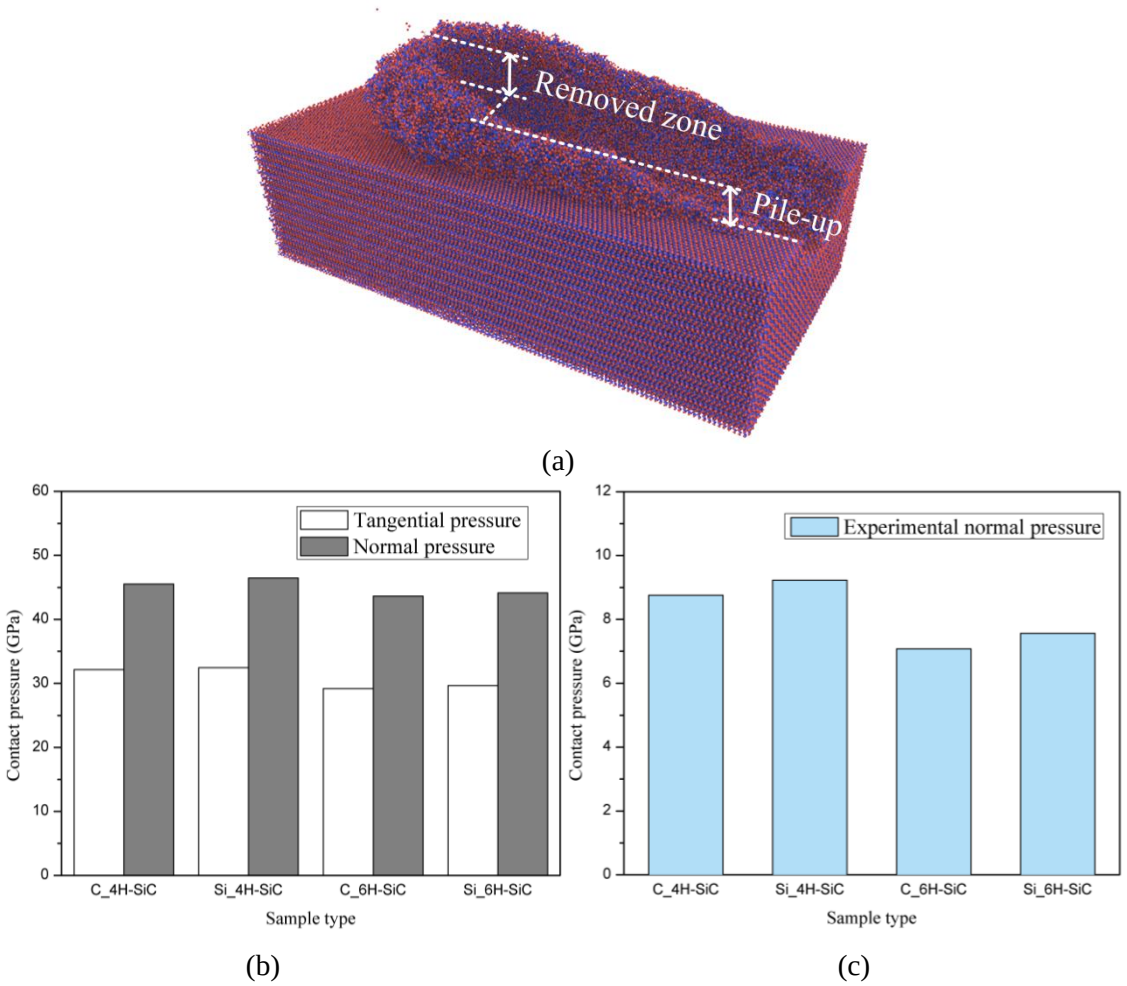

Figure 3. (a) Definition of removed atoms in nanoscale. (b) Numbers of displaced atoms above original surface. (c) Numbers of removed atoms.

4. Material deformation mechanism in abrasive scratching

4.1. Amorphisation behaviours in abrasive scratching

DXA is an analysis algorithm that can identify the defects in the lattice structure of a material. The basic concept underlying the DXA is the Burgers circuit construction, which is the canonical method to discriminate dislocations from other crystal defects and to decide their Burgers vectors. Here, the Burgers circuit C in analysis is a path in the dislocated crystal that composes of a sequence of atom-to-atom steps (line elements Δx) [28], and a mapping Δx→ Δx' is set up to translate each line element of the path to a corresponding image, Δx', in a perfect crystal lattice. Summing these transformed line elements algebraically along the associated path, C', gives the true Burgers vector of the dislocation enclosed by C [28]:

$$b = -\sum_{C'} \Delta x \tag{10}$$

The DXA can also identify dislocations, determine the Berkeley vectors and then depict them as dislocation lines within Ovito [29]. Figure 4 shows the MD simulation results obtained by using the

DXA, where the gray atoms represent amorphous atoms, and the blue and orange atoms indicate the standard lattice structures that represent cubic diamond structure and hexagonal diamond structure respectively. The ductile-regime machining at the nano-scale can be illustrated by the combination of structural transformation and atom dislocation activities [31]. The structural transformation took place in 6H-SiC was considered to be an amorphous transformation [11]. During scratching, disordered atoms form amorphous atom structures and lose regular lattice structures. Therefore, the amorphous atoms are considered to be the main subsurface defects, which could affect the properties of the material. From figure 4, it can be seen that horizontal slips or crystal dislocations appear below the abrasive contact zone. Although the maximum depths of amorphous deformation in four cases are similar, the subsurface amorphous layer of C face is relatively flat, while that of Si face is uneven for both 4H-SiC and 6H-SiC.

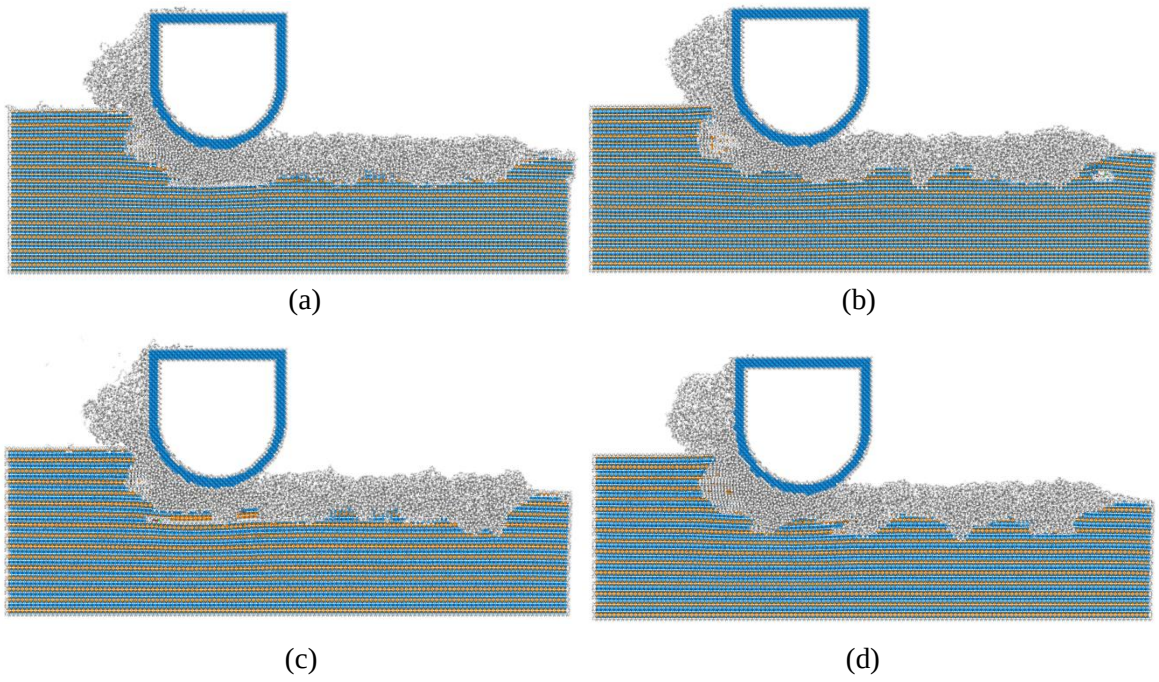

Figure 4. DXA analysis results. (a) C face of 4H-SiC, (b) Si face of 4H-SiC, (c) C face of 6H-SiC, (d) Si face of 6H-SiC.

In Figure 5 (a), the numbers of amorphous atoms in four different cases presented in Figure 4 were counted. It is interesting to see that fewer amorphous atoms appear at the C face than at the Si face for both materials of 4H-SiC and 6H-SiC. Therefore, the C face presents a better subsurface quality and less subsurface amorphous deformation than the Si face under the same machining conditions. Such a phenomenon is consistent with Luo's experimental investigation [20].

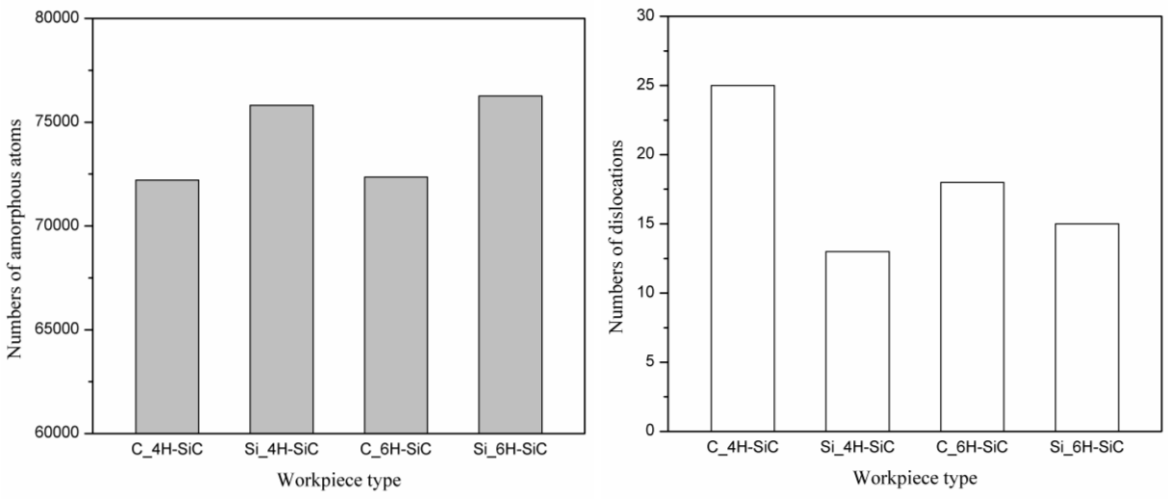

(a) (b)

Figure 5. Numbers of (a) amorphous atoms and (b) dislocations in subsurface.

4.2. Dislocation behaviours in abrasive scratching

Besides amorphous atoms formation during scratching, atom dislocations could happen. The DXA can also identify atom dislocation occurrence. Atom dislocations are often considered a form of plastic deformation, so in the analysis of DXA, the dislocations are only possible for atoms with regular lattice structures [28]. Figure 5b shows the number of dislocations in subsurface exists in all cases under the consideration. It can be seen that the number of dislocations generated during scratching the C face is greater than or even twice to that on the Si face.

Here, a scratching of 6H-SiC is selected to investigate the occurrence of dislocations. Figure 6 shows the morphology of subsurface deformation on Si face and C face of 6H-SiC. The DXA was used to judge the occurrence of dislocation. It can be seen that dislocations and slips mainly occur on the (0001) basal plane (clear under C face) and (10-10) plane (clear under Si face). The dislocations obtained in the MD simulation of Wu [11] are mainly on the (0001) and (11-22) planes. This difference may be associated with the limitation of Wu's MD model that only considered 2.58 nm in the y direction [11], which is too narrow to reveal the dislocations in the planes that is perpendicular to the y axis.

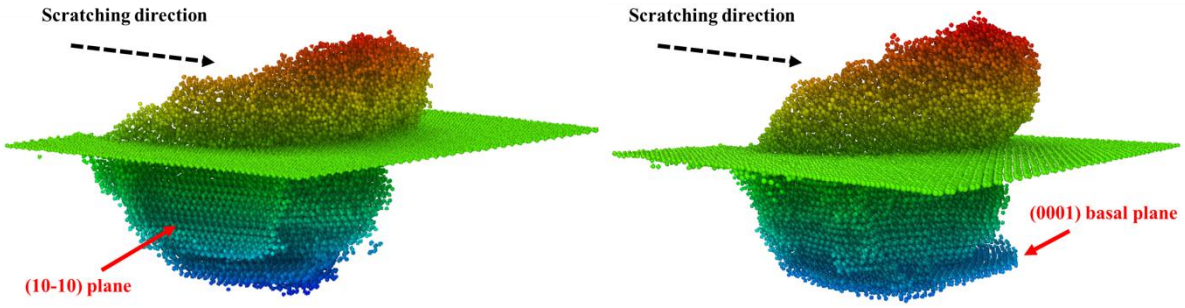

(a) (b)

Figure 6. Subsurface morphology of deformation on (a) Si face of 6H-SiC and (b) C face of 6H-SiC.

Particularly, for the C face, the dislocations are prone to occur on the basal plane (0001), while for the Si face, dislocations are easy to occur on the (10-10) plane during scratching. These dislocations

will lead to the slips along the scratching direction. In contrast with amorphous deformation, aligned dislocations and slips on the basal plane could reduce cutting force in material removal and promote better subsurface quality. In contradiction, those dislocations and slips on the (10-10) plane will lead to severe cracks in the subsurface layer, which explains the reason why more uneven irregular surfaces on the Si face than on the C face as mentioned before.

Figure 7 shows the scratching force smoothened by applying a moving average of 30 data reading spans (i.e. 0.3 nm) that filters off high frequency noise. Initially, the forces on both C and Si faces increase in almost the same trend. After the process enters into the stable scratching stage, the force on Si face still fluctuates while that on C face is much more stable. Such a phenomenon indicates that dislocations under C face during scratching tends to release stress in subsurface. As a result, the scratching force on C face becomes lower and more stable than that on Si face, therefore less amorphous atoms appear in the subsurface of C face, which is a clear evidence in Figure 5.

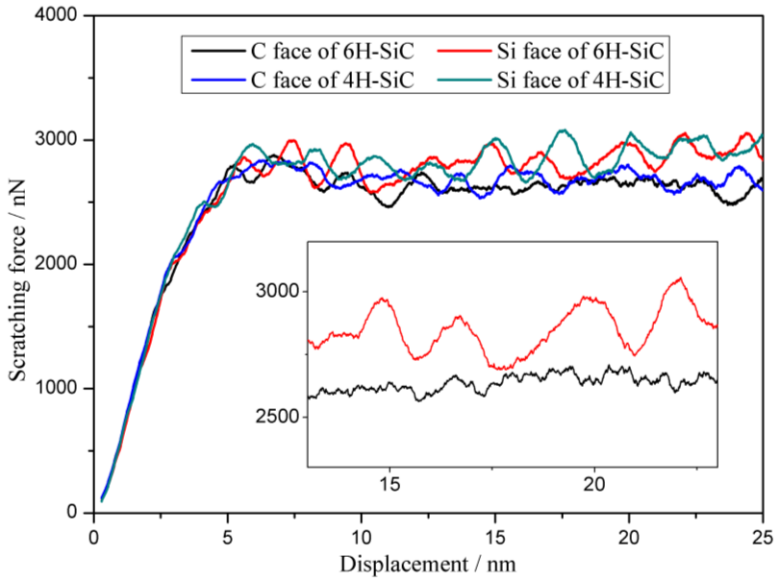

Figure 7. Scratching forces on C face and Si face of 4H- and 6H-SiC under the depth of cut of 3 nm.

5. Conclusions

In this paper, a series of MD simulations were performed on the C face and Si face of 4H-SiC and 6H-SiC scratching, aiming at the understanding of the mechanism of material removal and the formation of subsurface amorphous layer. The following conclusions are summarised:

1. Scratching simulation reveals that the dislocations and slips in SiC substrate occurs at both C face and Si face, mainly on the (0001) basal plane and the (10-10) plane.
2. Dislocations and slips on the (0001) plane are beneficial to material removal, which are more likely to appear on the C face than the Si face. For this reason, lower scratching forces and fewer amorphous atoms become evidence on the C face rather than on the Si face of SiC.
3. For SiC sample polishing, the quality of the C face could be better than Si face due to the C face structure prone to the (0001) basal plane dislocation or slip leading to less subsurface amorphous deformation appears on the C face.
4. Dislocations and slips at the (10-10) plane may promote material split to deep layer, which should be avoided.
5. Material removal at the C face is more efficient than that at the Si face.

Acknowledgements
The authors acknowledge financial supports from the Postgraduates' Innovative Fund in Scientific Research of Huaqiao University (No. 18011080010) and the National Natural Science Foundation of China (Grant No.51835004 and 51575197).

References
[1] Goel S 2014 The current understanding on the diamond machining of silicon carbide *J. Phys. D: Appl. Phys.* **47** 243001
[2] Perrone D 2007 Process and Characterisation Techniques on 4H- Silicon Carbide *Micronanotechnology, Ph. D. thesis, Politecnico di Torino, Torino, Italy.*
[3] Meng B, Zhang Y and Zhang F 2016 Material removal mechanism of 6H-SiC studied by nano-scratching with Berkovich indenter *Appl. Phys. A* **122** 247
[4] Zhou Y, Pan G, Shi X, Gong H, Luo G and Gu Z 2014 Chemical mechanical planarization (CMP) of on-axis Si-face SiC wafer using catalyst nanoparticles in slurry *Surf. Coat. Technol.* **251** 48-55
[5] Demenet J L, Amer M, Tromas C, Eyidi D and Rabier J 2013 Dislocations in 4H- and 3C-SiC single crystals in the brittle regime *Phys. Status Solidi C* **10** 64-67
[6] Ravindra D and Patten JA 2011 Chapter 4: Ductile regime material removal of silicon carbide (SiC). Silicon carbide: new materials, production methods and application **1** 141-167
[7] Goel S, Yan J, Luo X and Agrawal A 2014 Incipient plasticity in 4H-SiC during quasistatic nanoindentation. Journal of the mechanical behavior of biomedical materials **34** 330-337.
[8] Li Z, Zhang F and Luo X 2018 Subsurface damages beneath fracture pits of reaction-bonded silicon carbide after ultra-precision grinding *Appl. Surf. Sci.* **448** 341-350
[9] Grim J R, Benamara M, Skowronski M, Everson W J and Heydemann V D 2006 Transmission electron microscopy analysis of mechanical polishing-related damage in silicon carbide wafers *Semicond. Sci. Technol.* **21** 1709
[10] Luo X, Goel S and Reuben R L 2012 A quantitative assessment of nanometric machinability of major polytypes of single crystal silicon carbide *J. Eur. Ceram. Soc.* **32** 3423-3434
[11] Wu Z, Liu W and Zhang L 2017 Revealing the deformation mechanisms of 6H-silicon carbide under nano-cutting *Comput. Mater. Sci.* **137** 282-288
[12] Kang C, Tang J, Li L, Pan H, Xu P, Wei S, Chen X and Xu X 2012 In situ study on the electronic structure of graphene grown on 6H-SiC (000-1) with synchrotron radiation photoelectron spectroscopy *Appl. Surf. Sci.* **258** 2187-2191
[13] Hu Y, Zhang Y, Guo H, Chong L and Zhang Y 2016 Preparation of few-layer graphene on on-axis 4H-SiC (000-1) substrates using a modified SiC-stacked method *Mater. Lett.* **164** 655-658
[14] Pan G, Zhou Y, Luo G, Shi X, Zou C and Gong H 2013 Chemical mechanical polishing (CMP) of on-axis Si-face 6H-SiC wafer for obtaining atomically flat defect-free surface *J. Mater. Sci.: Mater. Electron.* **24** 5040-5047
[15] Chen G, Ni Z, Xu L, Li Q and Zhao Y 2015 Performance of colloidal silica and ceria based slurries on CMP of Si-face 6H-SiC substrates *Appl. Surf. Sci.* **359** 664-668
[16] Kim H M, Oh J E and Kang T W 2001 Preparation of large area free-standing GaN substrates by HVPE using mechanical polishing liftoff method *Mater. Lett.* **47** 276-280
[17] Shi X, Pan G, Zhou Y, Gu Z, Gong H and Zou C 2014 Characterization of colloidal silica abrasives with different sizes and their chemical–mechanical polishing performance on 4H-SiC (0001) *Appl. Surf. Sci.* **307** 414-427
[18] Kubota A, Yoshimura M, Fukuyama S, Iwamoto C and Touge M 2012 Planarization of C-face 4H-SiC substrate using Fe particles and hydrogen peroxide solution *Precis. Eng.* **36** 137-140
[19] Chen X, Xu X, Hu X, Li J, Jiang S, Ning L, Wang Y and Jiang M 2007 Anisotropy of chemical mechanical polishing in silicon carbide substrates *Mater. Sci. Eng. B* **142** 28-30
[20] Lu J, Luo Q, Xu X, Huang H and Jiang F 2019 Removal mechanism of 4H-and 6H-SiC

substrates (0001 and 000-1) in mechanical planarization machining *Proc. Inst. Mech. Eng., Part B* **233** 69-76
[21] Luo Q 2018 Research on Abrasive Polishing Removal Mechanisms of LED Substrates Materials *Ph. D. thesis, Huaqiao University, Xiamen,China.*
[22] Yagi K, Murata J, Kubota A, Sano Y, Hara H, Okamoto T, Arima K, Mimura H and Yamauchi K 2008 Catalyst-referred etching of 4H-SiC substrate utilizing hydroxyl radicals generated from hydrogen peroxide molecules *Surf. Interface Anal.* **40** 998-1001
[23] Tersoff J J 1989 Modeling solid-state chemistry: Interatomic potentials for multicomponent systems *Phys. Rev. B* **39** 5566
[24] Goel S, Luo X, Reuben R L and Rashid W B 2011 Atomistic aspects of ductile responses of cubic silicon carbide during nanometric cutting *Nanoscale Res. Lett.* **6** 589
[25] Zhang L and Tanaka H 1999 On the mechanics and physics in the nano-indentation of silicon monocrystals *JSME Int. J., Ser. A* **42** 546-559
[26] Goel S, Luo X, Agrawal A and Reuben R L 2015 Diamond machining of silicon: a review of advances in molecular dynamics simulation *Int. J. Mach. Tools Manuf.* **88** 131-164
[27] Plimpton S J 1995 Fast Parallel Algorithms for Short-Range Molecular Dynamics. *J. Comput. Phys.* **117** 1-19
[28] Stukowski A, Bulatov V V and Arsenlis A 2012 Automated identification and indexing of dislocations in crystal interfaces *Modell. Simul. Mater. Sci. Eng.* **20** 085007
[29] Stukowski A 2009 Visualization and analysis of atomistic simulation data with OVITO-the Open Visualization Tool *Modell. Simul. Mater. Sci. Eng.* **18** 015012
[30] Tian Z, Xu X, Jiang F, Lu J, Luo Q and Lin J 2019 Study on nanomechanical properties of 4H-SiC and 6H-SiC by molecular dynamics simulations *Ceram. Int.* **45** 21998-22006
[31] Meng B, Zhang Y and Zhang F 2016 Material removal mechanism of 6H-SiC studied by nano-scratching with Berkovich indenter *Appl. Phys. A* **122** 247